Geomechanics and Engineering, *Vol. 39, No. 4 (2024) 333-345*
https://doi.org/10.12989/gae.2024.39.4.333

An evaluation of the technical viability of employing combinations of xanthan gum and clay as an additive in Tunnel Boring Machine (TBM) slurries

Sojeong Lee[1a], Barrie Titulaer[2b], Hee-Hwan Ryu[3c] and Ilhan Chang*[4]

[1]*Korea Standard Construction Center, Korea Institute of Civil engineering and Building Technology, Goyang 10223, Korea*
[2]*Snowy Hydro, Cooma, NSW, 2630, Australia*
[3]*Next generation Transmission and Substation Laboratory, KEPCO Research Institute, Daejeon, 34056, Korea*
[4]*Department of Civil Systems Engineering, Ajou University, Su-won 16499, Korea*

(*Received May 9, 2024, Revised October 13, 2024, Accepted October 14, 2024*)

Abstract. The issue of problematic disposal of excavated material, commonly referred to as muck, generated during tunnel boring machine (TBM) excavation has emerged as an environmental challenge amidst the escalating demand for sustainable engineering solutions. TBM excavation operations necessitate the use of a slurry to bolster the excavation process and aid in muck conveyance. Typically composed of bentonite, this TBM slurry is conventionally discarded along with the excavated spoils, posing risks to human safety and raising environmental contamination apprehensions. This study aims to explore a novel slurry material as a means to mitigate the toxicity associated with muck disposal. Given the notable adsorption capabilities of bentonite, alternative options such as kaolinite clay and xanthan gum biopolymer are under consideration. Through experimental analysis, various combinations of bentonite clay, kaolinite clay, and xanthan gum are examined to assess their effectiveness in enhancing tunneling performance and optimizing transport properties. The evaluated parameters encompass rheological characteristics, swelling behavior, permeability, suspended viscosity and stickiness. Employing statistical analysis integrated with random weighting factors and the measured properties of each slurry candidate, competitiveness of each slurry candidate is analyzed. The findings of this investigation, accounting for 47.31% priority across all probabilistic scenarios, indicate that a specific blend consisting of bentonite and xanthan gum (2.5% bentonite, 0.75% xanthan gum) demonstrates considerable promise as a substitute for conventional bentonite-based slurries (7.5% bentonite) in TBM excavation applications.

Keywords: biopolymer; biopolymer-based soil treatment (BPST); geotechnical engineering; xanthan gum; slurry

1. Introduction

The full-face tunnel boring machine (TBM) stands as a prominent choice in contemporary underground construction endeavors, owing to its adept management of excavation volumes and minimized disruption to surrounding ground conditions. Particularly, the earth pressure balance (EPB) TBM and slurry shield (SS) TBM represent prevalent options for excavating soft soil terrains, each operating through distinct mechanisms. Statistics indicate that the utilization of SS TBM accounts for 46.3% of TBM construction projects, while EPB TBM deployments constitute 40.7% of total TBM implementations (Park *et al*. 2020). The EPB TBM ensures equilibrium of mechanical forces in counteracting earth pressure through its driving mechanism, whereas the SS TBM, commonly employed in substrates with high water content, counters earth pressure through hydraulic means by employing a slurry substance within the excavation chamber (Rostami *et al.* 2023). Both types of TBMs necessitate the utilization of a slurry (for SS TBM) or a conditioner (for EPB TBM) to uphold chamber pressure and facilitate the conveyance of excavated material. Typically, these slurries and conditioners predominantly consist of bentonite (Bernard *et al*. 2019). However, there has been a notable reluctance towards the utilization of bentonite, primarily attributed to emerging environmental apprehensions. Despite its widespread application in diverse geotechnical engineering contexts (Alther 1987, Jain 2024, Malusis *et al.* 2013, Yoon *et al*. 2020), the indiscriminate disposal of spent bentonite poses potential adverse effects on both human health and the surrounding ecosystem subsequent to its field deployment (Kubilay *et al.* 2007, Ouhadi *et al*. 2006). Indeed, bentonite-based drilling fluids undergo chemical alteration during drilling and recycling processes, leading to the release of hazardous substances (Broni-Bediako and Amorin 2010). These fluids, upon use, contain a range of caustic and toxic components including soda, soda phosphate, hydrated lime, sump oil, diesel, phenol, phenol derivatives, and barium sulfate, as bentonite absorbs various additives such as thinners (e.g., lignosulfonate or anionic polymers), filtrate control agents (e.g., carboxymethyl cellulose or starch), and lubrication agents (e.g., polyglycols) (Gardner 2003). Furthermore, sporadic disposal of excavated muck at Tunnel Boring Machine (TBM) sites, which often contains a significant

*Corresponding author, Associate Professor
E-mail: ilhanchang@ajou.ac.kr
[a]Ph.D. Post-Doctoral Researcher
[b]Graduate Engineer-Strategic Engineering
[c]Ph.D. Principle Researcher

ISSN: 2005-307X (Print), 2092-6219 (Online)

Table 1 Properties of clay used in this study

Clay	Kaolinite	Montmorillonite
D_{50} [um]	3	0.07
Specific surface area [m^2/g]	22.1	220.6
Cation exchange capacity [meq/100 g]	6.1	64.1
Plastic limit [%]	31	61.6
Liquid limit [%]	69.8	398.5
USCS	CH	CH

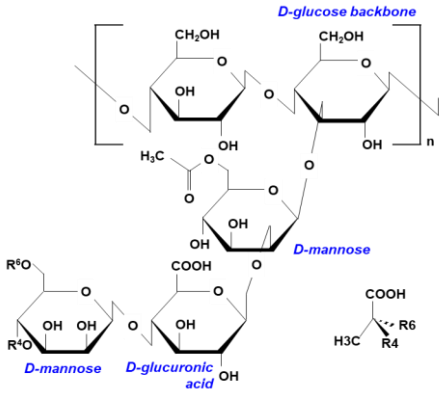

Fig. 1 Molecular structure of xanthan gum biopolymer.

proportion of contaminated bentonite, raises environmental concerns. Consequently, efforts have been made to reduce its usage through the incorporation of additives such as polyacrylic acid polymer, acrylates polymer, sodium bicarbonate, sulfuric acid, and soda ash (Swartz 2021). Studies suggest that the addition of 0.05% polymer (by mass ratio to water) can potentially reduce bentonite usage by approximately 30% (Fritz 2007). However, conventional additives have been associated with toxicity concerns; for example, sulfuric acid is classified as a carcinogen upon human exposure (New Jersey Department of Health 2016), and polyacrylic acid hydrogel has been linked to gastrointestinal irritation and neurotoxicity (Dorman *et al.* 2018). Therefore, the development of sustainable slurry additives holds promise for mitigating the toxicity associated with excavated materials.

The primary objective of this study is to assess the viability of employing a novel environmentally friendly additive material to reduce the reliance on chemical polymers in Tunnel Boring Machine (TBM) construction. Slurry shield TBMs are commonly employed in highly permeable ground conditions, with their effectiveness often contingent upon grain size considerations (Fritz 2007, Krause 1987). This study examines various combinations of kaolinite clay, bentonite clay, and xanthan gum (XG) biopolymer as potential additives. Notably, XG has been previously investigated for its technical feasibility in EPB-TBM applications as an excavation fluid additive (The French Association of Tunnels and Underground Space 2005). XG was evaluated as a sustainable additive owing to its ability to provide competitive strengthening effects alongside its environmentally friendly attributes. Indeed, biopolymer-based soil treatment (BPST) utilizing XG has recently garnered attention due to its broad range of geotechnical applications, including soil strengthening, ground improvement, erosion reduction, and drilling (including hydraulic conductivity control), all while emphasizing sustainability (Cabalar *et al.* 2017, Fu *et al.* 2022, Kwon *et al.* 2021, Latifi *et al.* 2016, Lee *et al.* 2019). Furthermore, the formation of a biopolymer-clay matrix is recognized as pivotal in enhancing soil properties such as liquid limit and undrained shear strength (Chang and Cho, 2019, Chang *et al.* 2019, Chang *et al.* 2021). XG possesses several desirable attributes highly valued in geotechnical engineering, notably its biodegradability, biocompatibility, and renewability, which can potentially contribute to reducing greenhouse gas emissions when compared to conventional soil binders (Chang *et al.* 2016, Chang *et al.* 2020, Lee *et al.* 2017).

Experimental programs were undertaken to assess the competitiveness of attempted slurry materials, with comparisons made against a conventional bentonite slurry. Evaluation criteria encompassed parameters such as apparent viscosity (η), yield point (τ_o), plastic viscosity (η_p), swelling pressure (p_s), permeability (k), suspended viscosity, and stickiness (λ). Inferential statistical analysis was employed, incorporating random weight factors for each measured parameter to ascertain superiority among the proposed slurry candidates. Optionally, cost considerations were integrated alongside the four primary measured parameters, namely yield point (τ_o), plastic viscosity (η_p), swelling pressure (p_s), and permeability (k).

Both the rheological and physical attributes hold significance in the evaluation of slurry materials. Ensuring the appropriate properties of slurry can guarantee excavation workability without clogging (Liu *et al.* 2023). The rheology and shear-thinning behavior of tunneling slurries are considered pivotal parameters influencing excavation efficiency, encompassing aspects such as tunnel face stabilization, groundwater control, muck removal, slurry preparation, and treatment performance (Cui *et al.* 2020b, Sun *et al.* 2018, Zhao *et al.* 2021). Shear thinning refers to the decrease in apparent viscosity (η) with increasing strain rate, a phenomenon observed in the viscous-elastic behavior of slurry materials during tunneling operations, where the transport and excavation velocities vary. Other crucial properties of slurry materials include swelling pressure (p_s), permeability (k), suspended viscosity (η_{sus}), and stickiness (λ). Similar to the importance of compressibility in EPB-TBM excavation, swelling pressure (p_s) plays a significant role as it indicates the appropriate range of pressure balance between earth pressure (including groundwater pressure) and supporting force along the excavation face. Permeability (k) of the slurry is essential for effective muck transport post-excavation, as it directly influences the flow characteristics from the excavation chamber to the discharge system. Suspended viscosity (η_{sus}) is a commonly used parameter for assessing slurry treatment systems, as it is influenced by the aggregation shape and particle interactions (Yoshida *et al.* 2013). Stickiness (λ) or clogging is another critical consideration,

Table 2 Summary of slurry materials and test methods used in this study

Slurry type	Symbols	Composition[1] (%)			Test Programs			
					Tunneling performance		Transportation performance	
		Bentonite	Kaolinite	Xanthan gum	Rheology (η, τ_o)	Permeability (k)	Suspended viscosity(η_{sus})[2]	Stickiness (λ)
B2.5		2.5	-	0.0	○	○	-	-
B2.5-XG0.75		2.5	-	0.75	○	○	○	○
B2.5-XG1.25		2.5	-	1.25	○	○	-	-
B5.0		5.0	-	0.0	○	○	-	-
B5.0-XG0.5		5.0	-	0.5	○	○	○	○
B5.0-XG1.0		5.0	-	1.0	○	○	-	-
B7.5		7.5	-	0.0	○	○	○	○
B10.0		10.0	-	0.0	○	○	○	○
K2.5		-	2.5	0.0	○	○	-	-
K5.0		-	5.0	0.0	○	○	-	-
K5.0-XG0.75		-	5.0	0.75	○	○	○	○
K5.0-XG1.0		-	5.0	1.0	-	-	-	-
K5.0-XG1.25		-	5.0	1.25	○	○	-	-
K7.5		-	7.5	0.0	○	○	-	-
K10.0		-	10.0	0.0	○	○	-	-
K10.0-XG0.5		-	10.0	0.5	○	○	○	○
K10.0-XG0.75			10.0	0.75	-	-	-	-
K10.0-XG1.0		-	10.0	1.0	○	○	-	-

1) Soliid to solution (i.e. slurry; clay+xanthan gum+water) ratio in mass.
2) 20% coarse soil (Sydney sand) and 10% fine soil (Queensland clay) suspended conditions were tested using a rheometer.

Table 3 Properties of clay used in this study

Slurry type	Bentonite [%]	Kaolinite [%]	Xanthan gum [%]
B100	100	-	0.0
B100-XG0.5	100	-	0.5
B100-XG1.5	100	-	1.5
K100	-	100	0.0
K100-XG0.5	-	100	0.5
K100-XG1.0	-	100	1.0
K100-XG2.0	-	100	2.0

impacting excavation efficiency as excavated soils are transported through the screw conveyor system of the EPB TBM or a slurry discharge pipe of the SS TBM.

2. Materials and Methods

2.1 Materials

2.2.1 Bentonite

Bentonite is a clay that mainly consists montmorillonite minerals and smectite minerals, where bentonite is generally originated via the chemical alternation of volcanic ash (Holtz *et al.* 2011). Montmorillonite exhibits a repeated structural composition of two silica layers and one alumina layer. Montmorillonite has a cation exchange capacity strong water absorption force since tops of silica sheets are connected by van der Waals' force resulting weak bonding compared with hydrogen bonding of kaolinite. Additionally, montmorillonite renders high cation exchange capacity (CEC) correspondingly. In this study, research-grade bentonite was used (Sigma–Aldrich, CAS number: 1302-78-9; CEC = 64.1 meq/100 g), where the basic properties of bentonite (montmorillonite) are summarized in Table 1.

2.2.2 Kaolinite

Kaolinite clay originates from the weathering of feldspar and mica in granitic rocks; it exhibits a repeated skeletal structure comprising one silica layer and one alumina layer (Holtz et al. 2011). Each skeletal structure is connected via hydrogen bonding between the silica and alumina layers. The strong hydrogen bonding results in less hydration and swelling compared to bentonite (montmorillonite). Research-grade kaolinite (Walker Ceramics, CAS number: 1332-58-7) was used in this study and its basic properties are summarized in Table 1.

2.2.3 Xanthan gum

Xanthan gum (XG; $C_8H_{14}Cl_2N_2O_2$) is an extracellular polysaccharide biopolymer produced from Xanthomonas campestris. The main structure of XG shows a repeating cellulosic backbone with side chains comprising two mannoses and one glucuronic acid as shown in Fig. 1 (García-Ochoa *et al.* 2000). XG forms a hydrophilic hydrogel in the form of negatively charged carboxyl groups (COO^-) on the side chains when it dissolves in water (Phillips and Williams, 2000). Intermolecular interaction of

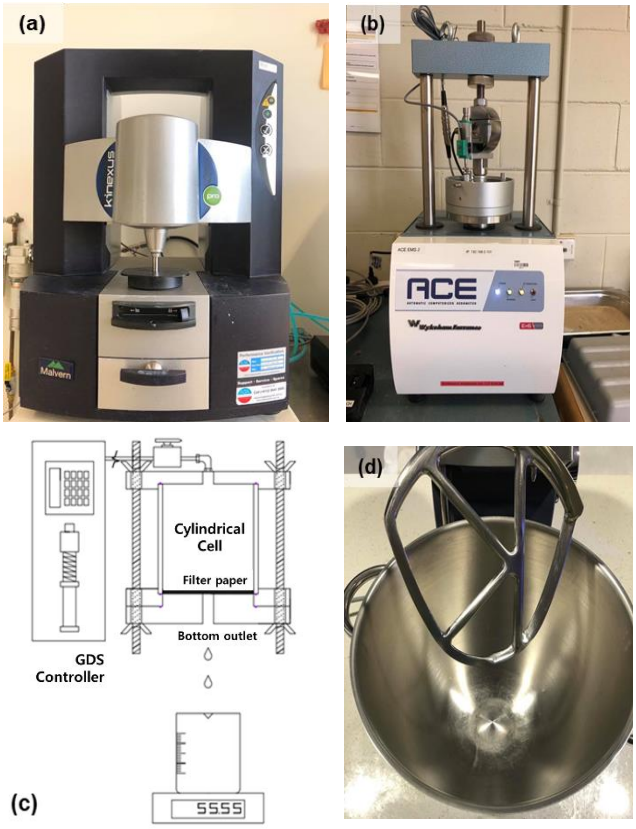

Fig. 2 Each test method of experimental programs

XG in a dissolved solution induces pseudoplasticity (e.g., shear thinning). XG has been widely applied in various industrial fields due to its pseudo-plasticity, viscosity, and high stability within a wide range of temperatures and pH conditions (García-Ochoa *et al.* 2000, Katzbauer 1998). In geotechnical engineering, XG is recently being considered as a new soil stabilization and strengthening material (Chang *et al.* 2015, Lee *et al.* 2019, Lee *et al.* 2021). In this study, research-grade XG (Sigma–Aldrich, CAS number: 11138-66-2) was used for laboratory tests.

3. Experimental program

3.1 Specimen preparation

Common slurry materials contains 3%–8% of bentonite depending on the ground condition in practice (Swartz 2021), thus, bentonite 7.5% condition (B7.5) is regarded as a common slurry type in this study. For comparison, different slurry mixtures (kaolinite, bentonite, kaolinite + xanthan gum, bentonite + xanthan gum) have been considered. The detail configuration of each slurry type is summarized in Tables 2 and 3. Four different concentrations were chosen for pure bentonite and pure kaolinite slurry types as 2.5%, 5.0%, 7.5%, and 10.0% in a mass ratio to water since B7.5 was assumed as a common slurry configuration. The bentonite-based hybrid (hereinafter B+XG) slurries consisted of 2.5% and 5.0% of bentonite clay (clay to slurry ratio in mass), while kaolinite-based hybrid (hereinafter K+XG) slurries contained 5.0% and 10.0% kaolinite clay according to their adequate shear thinning behavior. The less amount of XG biopolymer was added to higher concentration of pure clay slurries to ensure shear thinning property. Each slurry type was prepared by dissolving xanthan gum powder and dry clay into water using an electric hand mixer for homogeneous mixing. In this study, the XG hydrogel was tested without resting time to ensure that shear thinning property governs XG hydrogel (Ong *et al.* 2019, N'gouamba *et al.* 2021). Tunneling performance indices (i.e., η, τ_o, and k) were mainly considered, while the tests for transport characteristics (i.e., η_{sus} and λ) were limited to B2.5-XG0.75, B5.0-XG0.5, B7.5, B10.0, K5.0-XG0.75, K10.0-XG0.5 cases which showed competitive tunneling performance (in terms of η, τ_o, or k) compared to the B7.5 reference (Table 2). The experimental cases for the swelling assessment are summarized in Table 3.

3.2 Experimental methods

3.2.1 Apparent viscosity (η)/ yield point (τ_o) measurement

As clay-based slurries and XG hydrogels are non-Newtonian (i.e., shear thinning) fluids, the η was assessed with a dynamic shear rheometer (Malvern Kinexus Pro Rheometer) (Fig. 2(a)). A bottom plate with a diameter of 65 mm and an overlaying parallel plate-shaped rotating spindle with a diameter of 50 mm were selected and calibrated with glycerin. Freshly prepared slurry specimen was placed on the bottom plate, and the adjustment between the bottom plate and spindle was set to 2 mm. Following that, side residues were trimmed to prevent data distortion from overfilling. The experiment was conducted under strain (shear) rate control ranging from 0.001 to 1000 s^{-1}. The temperature was set to 25°C, and each test condition was repeated three times for data accuracy. The overall test procedure followed ASTM D7175 (ASTM 2015).

In this study, rheological properties, η, η_p, and τ_o were mainly considered. η_p is a common parameter for drilling fluids which represents the gradient of the shear stress change with shear strain. τ_o is associated with the flow behavior in a non-Newtonian fluid, where τ_o represents the threshold point of fluid liquidity. In other words, τ_o is used to determine whether fluid behaves like solid or liquid. A slurry that flows easily improves transportation efficiency, whereas a slurry with a high viscosity is recommended to facilitate the accumulation of excavated spoils (The French Association of Tunnels and Underground Space, 2005). In practice, a lower η is preferred to improve the slurry transport during construction, while slurry viscosity varies throughout the construction stage emphasizing the importance of precise quality control.

3.2.2 Swelling test

The swelling potential was assessed via an automatic oedometer apparatus (Wykeham Farrance; ACE 26-WF0320) in accordance with ASTM D 4546-14 (ASTM 2021) (Fig. 2(b)). Each test specimen was placed into a consolidation cell (50 mm in diameter). The initial

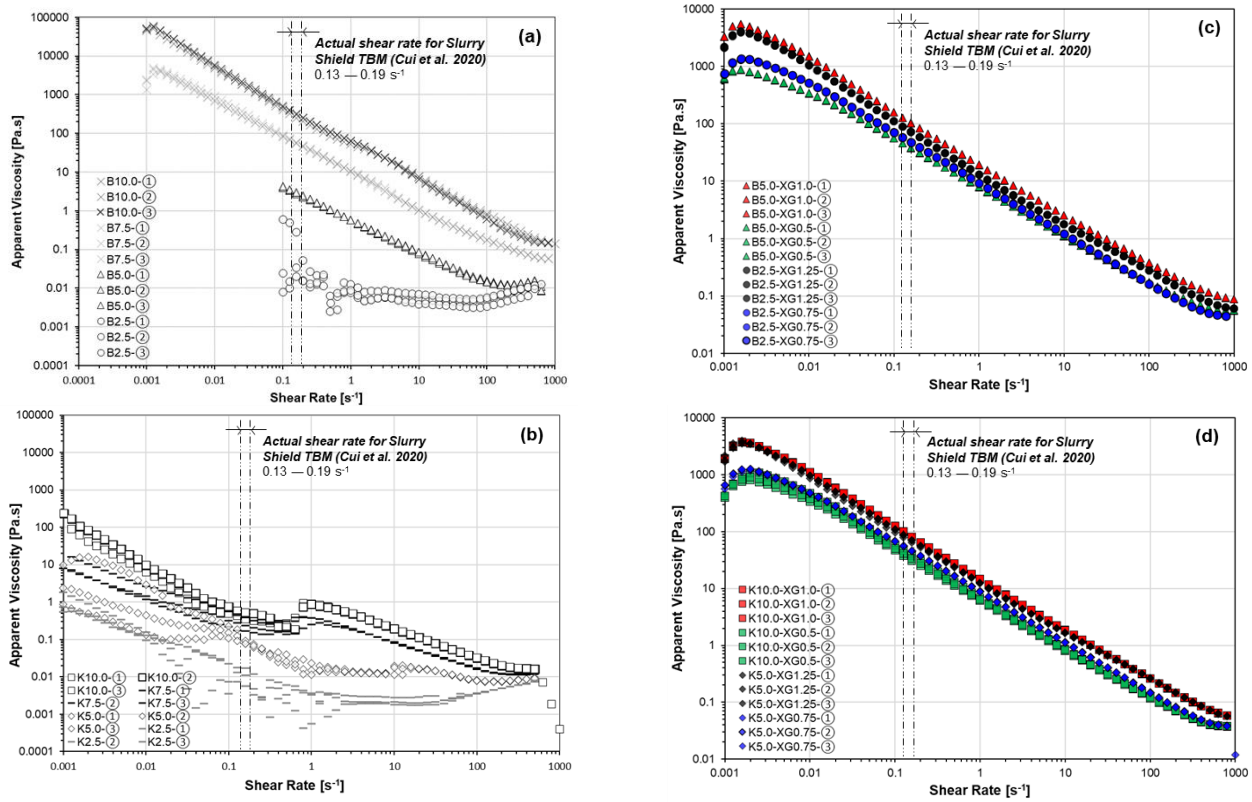

Fig. 3 Apparent viscosity (η) of pure clay slurry types and hybrid slurry types

specimen height was set at 12 mm without compaction. Thereafter, an initial overburden stress of 6.25 kPa was applied. When no more settlement has been observed, water was poured to allow specimen saturation and the corresponding volume expansion was monitored by a LVDT (Linear Variable Displacement Transducer) attached to the top of the consolidation cell. After the volumetric swelling assessment, subsequent consolidation loading was conducted following the loading sequence of 6.25, 10, 20, 50, 100, 200, 400 kPa. The maximum loading pressure for kaolinite and kaolinite-XG hybrids was 200 kPa, while it was 400 kPa for bentonite and bentonite-XG hybrids. Each test configuration was repeated twice for data accuracy.

3.2.3 Permeability (k) test

A modified low-pressure filter-press device was fabricated to assess *k* of the slurry by referring to Blkoor and Fattah (2013). The modified low-pressure filter-pressure device used in this study (Fig. 2(c)) composes a cylindrical cell a digital pressure controller (GDS STDDPC). The cylindrical cell to contain slurries was fabricated with acryl having dimensions as 100 mm in diameter and 100 mm in height. A filter paper (GE Healthcare Life Science Whatman® grade 40) was placed at the bottom of the cylindrical cell, and 250 mL of the slurry specimen was poured into the cell. A back pressure of 250 kPa was applied using a digital pressure controller, where the back pressure level was selected referring to typical range (150 to 300 kPa) used in previous studies (Dias and Bezuijen 2015, Park *et al.* 2018, Shirlaw *et al.* 2009). Water discharged through the slurry was collected from the bottom outlet and the volume was measured every 2 seconds.

In practice, SS TBM is typically used for soft grounds with high in-situ water contents where a lower k (10^{-4} <k < 5×10^{-4} m/s) of fresh slurry is preferred as low permeable filter cake is highly likely to minimize fluid loss into permeable ground (Fritz 2007, Kelessidis *et al.* 2007).

3.2.4 Suspended viscosity (η_{sus})

Several research have attempted to evaluate the rheological property, specifically η_{sus}, via theoretical derivations such as Einstein, modified Simha (Simha, 1952), Mooney (Mooney 1951), and Thomas equations (Thomas 1965). However, theoretical evaluations are insufficient to explain the rheological behavior of slurry with suspended particles. Therefore, η_{sus} was intuitively measured experimentally in a previous study (Yoshida *et al.* 2013).

As suspended viscosity (η_{sus}) is analogous to rheology testing, η measurement and η_{sus} measurement are similar. The explicit difference of η_{sus} is that spoil (i.e., 20% of coarse soil (CS) or 10% of fine soil (FS) by mass ratio) is added to the slurry and slurry materials were considered in this study (i.e., pure bentonite slurry, B+XG slurry, and K+XG slurry). In details, B7.5, B10.0, B2.5-XG0.75, B5.0-XG0.5, K5.0-XG0.75, and K10.0-XG0.5 were considered (Table 2). Sydney sand (D_{30} = 0.31 mm; D_{50} = 0.39 mm; C_u = 2.35;

C_c = 1.45; G_s = 2.65; e_{max} = 0.77; e_{min} = 0.57; USCS = SP) and Queensland clay (LL = 59.6; PL = 27.8; PI = 31.8) (Rankine, 2007) were used as coarse soil spoil and fine soil spoil, respectively. Each configuration was repeated three times, and the resulting average data were plotted.

3.2.5 Stickiness (λ) testing

As XG hydrogels render high viscosity, the λ has been an important consideration for the newly attempted slurry materials in this study. λ is associated with clogging of muck during tunneling, where previous studies have proposed quantitative measurement methods to evaluate λ. Followed by previous studies with quantitative measurement methods (Feinendegen *et al.* 2010, Peila *et al.* 2016), Zumsteg *et al.* (2016) assessed λ of slurries containing a soil conditioner rather than relying on conventional intuitive prediction.

In this study, the λ of slurry and spoil mixtures was measured referring to Zumsteg and Puzrin (2012). A Hobart mixer with a mixing paddle was used (Figure 2d). Six slurry candidates – B2.5-XG0.75, B5.0-XG0.5, B7.5, B10.0, K5.0-XG0.75, K10.0-XG0.5 were tested. In details, 1000 g of slurry, and 200 g of fine spoil (Queensland clay) were prepared by homogeneous mixing. Queensland clay was prepared by breaking it with a mortar and pestle and sieving it through a #200 US standard sieve (75 μm).

Subsequently, its λ was determined as follows

$$\lambda = \frac{G_{MT}}{G_{TOT}} \tag{1}$$

where G_{MT} refers to the weight of soil adhered to the mixing tool, and G_{TOT} is the total weight of soil in the mixer. This empirical parameter was selected because a quantitative comparison of slurries is intrinsically available.

4. Result and discussion

4.1 Plastic viscosity/yield point

Pure bentonite slurries (B5.0, B7.5, and B10.0 — Bentonite 5.0%, 7.5%, 10.0% in a mass ratio to water) exhibit non-Newtonian fluid shear thinning behavior, except B2.5 (Bentonite 2.5% in a mass ratio to water) as shown Fig. 3(a). In contrary, pure kaolinite slurries (K2.5, K5.0, K7.5, and K10.0 — Kaolinite 2.5%, 5.0%, 7.5%, 10.0% in a mass ratio to water) show unstable shear thinning behavior compared to B5.0, B7.5, and B10.0 slurries (Fig. 3(b)).

Adding XG to the clay slurries within a small amount as $m_{biopolymer}/m_{slurry}$ from 0.5 to 1.25% significantly enhanced the viscosity of clay slurries regardless of the clay type (Figs. 3(c) and 3(d)). Even though pure kaolinite slurries have shown insufficient shear thinning, K+XG slurries (Kaolinite + XG biopolymer blends) exhibited an improved η value (Fig. 3(c)) similar to that of B+XG slurries (Bentonite + XG biopolymer blends) (Figs. 3(c) and 3(d)). In fact, the η of the K+XG slurries increased up to approximately ten times that of the 10% pure kaolinite slurry.

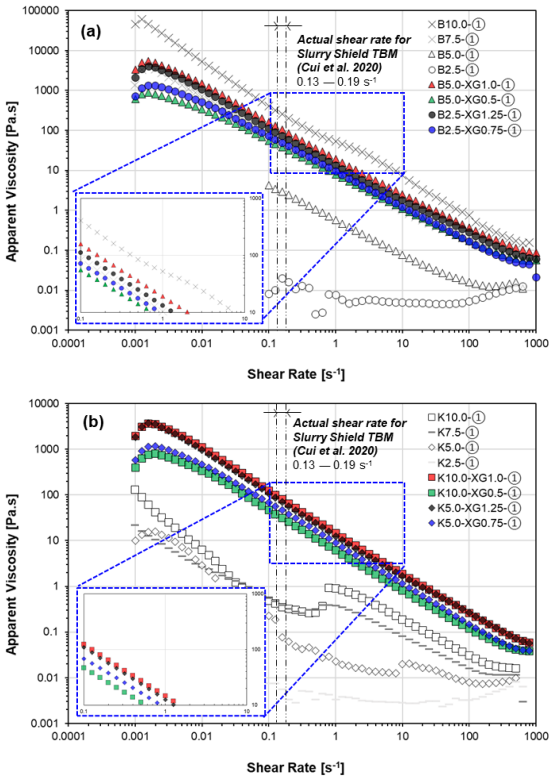

Fig. 4 Potential of hybrid slurries in terms of apparent viscosity (η)

Regarding the engineering properties of B7.5 slurry to be appropriate measures, XG treatment renders sufficient shear thinning behaviors as shown in Fig. 4. With XG treatment, the shear rate-apparent viscosity relationship of both B2.5-

XG and B5.0-XG slurries become similar to that of B7.5 slurry, regardless of XG content (Fig. 4(a)). The XG treatment becomes more effective for K slurries, where the K+XG slurries all show clear shear thinning trends (Fig. 4(b)), unlike the inconsistent pure K slurries (Fig. 3(b)).

In practice, the common shear rate for SS-TBM excavation is reported as 0.13–0.19 s^{-1} (Cui *et al.* 2020a). As marked in Figs. 3 and 4, the η values of both B+XG and K+XG slurries are improved to that of reference slurry (B7.5), which are adequate for TBM excavation practices.

In terms of yield point (τ_o), despite the τ_o of B2.5 slurry is unmeasurable, τ_o becomes countable with higher bentonite contents as 0.45 Pa (B5.0), 1.1 Pa (B7.5), and 7 Pa (B10.0), while τ_o of B+XG slurries become similar to that of B7.5 even though the bentonite content was low (B2.5) (Figure 5a). XG treatment becomes more effective for K slurries, where the τ_o values of K+XG slurries are improved and become accordant to the B7.5 and B+XG slurries in terms of τ_o and η (Fig. 5(b)).

The addition of XG enhances the shear thinning behavior in B+XG and K+XG slurries, where the viscosity properties (i.e., η, τ_o, and η_p) of K+XG and B+XG slurries become similar to those of B7.5 slurry. In addition, a small amount of XG treatment narrows the viscosity differences between B2.5, B5.0, B7.5, and B10.0 slurries, whereas

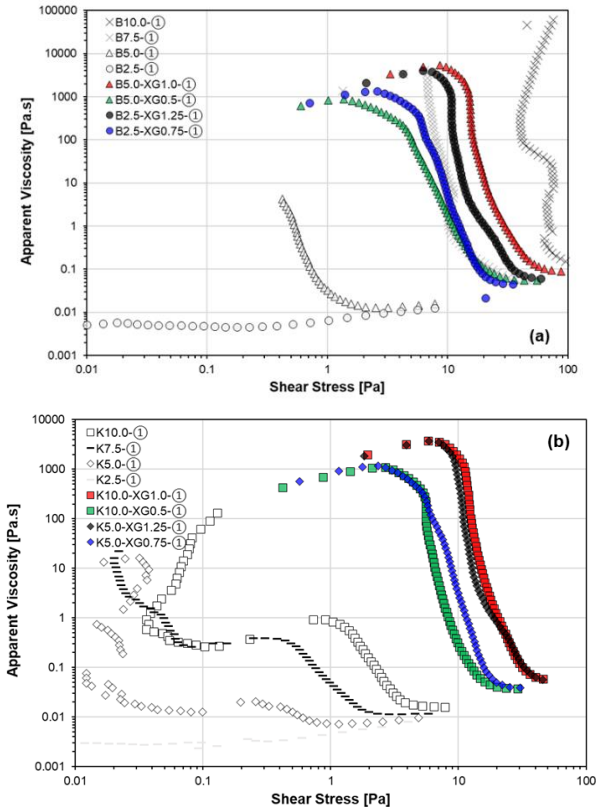

Fig. 5 Potential of hybrid slurries in terms of yield point (τ_o)

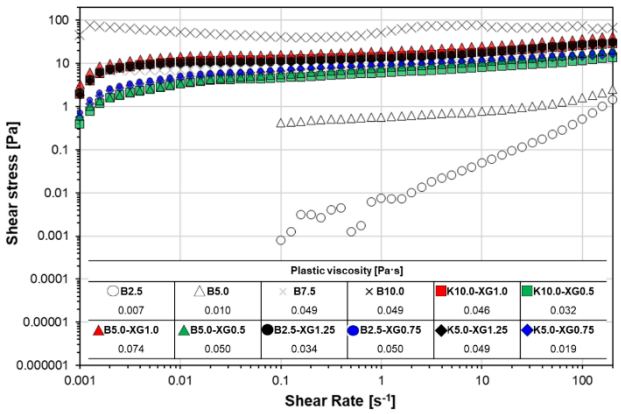

Fig. 6 Potential of hybrid slurries in terms of plastic viscosity (η_p)

renders K+XG slurries to have a clear shear thinning behavior unlike natural kaolinite slurries. The increment in η_p in the pure B-slurries was noticeable in the 2.5% to 7.5% bentonite suspension range.

In detail, η_p increased from 0.0074 Pa·s (B2.5), 0.0104 Pa·s (B5.0), to 0.0486 Pa·s (B7.5) with bentonite content increase, while B10 slurry was extremely viscous and behaved like colloidal solid (Fig. 6). Most B+XG and K+XG slurries have shown similar or higher η_p values than B7.5 (η_p = 0.049) and B10.0 (η_p = 0.048) except B2.5-XG0.75, K10.0-XG0.5, and K5.0-XG0.75. All B+XG and K+XG slurries satisfied the requirement for drilling fluids,

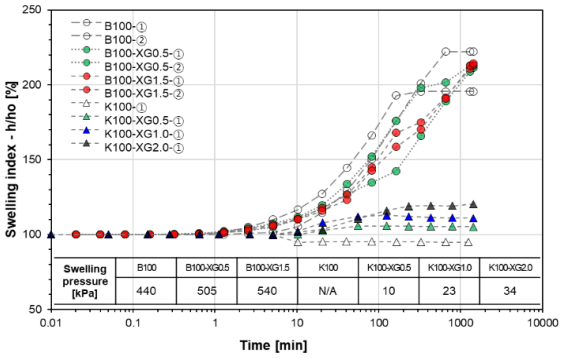

Fig. 7 Swelling behavior measured based on volumetric change

where the American Petroleum Institute (API) recommends the η_p of bentonite-base drilling fluid to be η_p > 0.01 Pa·s (American Petroleum Institute, 2020).

4.2 Swelling pressure (p_s)

Fig. 7 depicts the swelling pressure (p_s) test results for B-, K-, B+XG, and K+XG slurry mixtures. The swelling index (%) in Fig. 7 represents the volumetric strain (swelled volume / initial volume) according to specimen saturation. Pure bentonite (B100) showed 100% of volume expansion via saturation, which results to p_s = 440 kPa. The high swelling index and p_s of bentonite attribute to the high specific surface area and water absorption capacity of montmorillonite minerals (Holtz *et al.* 2011). Despite XG treatment increases the ps of B+XG slurries, the improvement effect is less noticeable than K+XG slurries (Fig. 7), where XG is regarded to mainly aggregate montmorillonite particles rather than altering the viscosity of pore fluids (Chang *et al.* 2019).

In contrary, pure kaolinite (K100) showed volumetric compression (approximately 5%) when saturated by water (Fig. 7). However, the compressive behavior of kaolinite turned to volumetric swelling when XG was added, where the swelling index and p_s increased with XG content increase as: 10 kPa (K100-XG0.5), 23 kPa (K100-XG1.0), and 34 kPa (K100-XG2.0) (Fig. 6). The swelling behavior of K+XG slurries imply the pore fluid viscosity thickening induced by XG (Chang *et al.* 2019).

4.3 Permeability (k)

Fig. 8(a) shows that the k of B2.5, B5.0, B7.5, and B10.0 slurries, where k gradually decreases with higher bentonite contents. In particular, the filtrate volume for the B2.5 was 53.18 mL during 30 mins (k = 4.70 × 10^{-6} m/s), while the filtrate volume for B10 was 13.5 mL during the same time (k = 1.21 × 10^{-6} m/s). The k values for kaolinite suspensions also decreased from 114.41 × 10^{-6} m/s (K2.5) to 35.20 × 10^{-6} m/s (K10.0) with kaolinite content increase (Fig. 8(b)). The k values of pure kaolinite slurries were remarkably higher than the k of pure bentonite slurries. The k values of bentonite suspensions were around 25 to 30 times higher than the k values of kaolinite suspensions at the same clay content conditions (i.e., k ratios between B

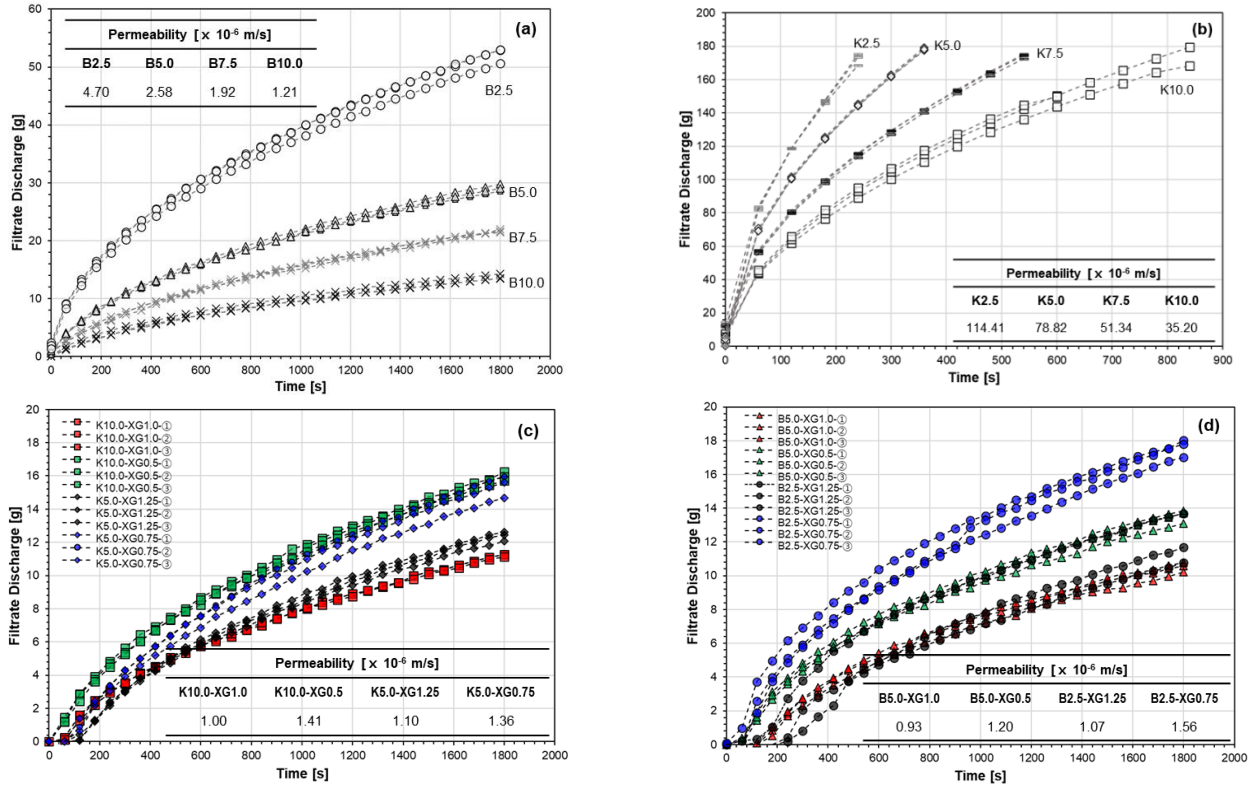

Fig. 8 Permeability (k) of slurries under confined pressure

and K are: B2.5/K2.5 = 24.3, B5.0/K5.0 = 30.6, B7.5/K7.5 = 26.7, and B10/K10 = 29.1) (Fig. 8(b)). Meanwhile, the k of all B+XG and K+XG slurries were lower than that of B7.5 (k = 1.92 × 10^{-6} m/s), as shown in Figs. 8(c) and 8(d). XG treatment rendered a high amount of k reduction, for example, the k of K10.0 (k = 35.20 × 10^{-6} m/s) dropped to 1.41 × 10^{-6} m/s (K10.0-XG0.5) and 1.00 × 10^{-6} m/s (K10.0-XG1.0). The k reduction with XG content in the same amount of clay suspension implies higher efficiency of filter cake formation due to the XG-clay matrix formation induced by XG hydrogels (Chang and Cho 2019, Chang *et al.* 2021). Filter cake is usually formed by clay particle transportation to the ground at the face to maintain pressure balance. It was reported that a filter cake is commonly formed through clogging and following consolidation (Min *et al*. 2013). While a thin filter cake is favorable for high excavation efficiency, a thick filter cake is commonly formed when flocculates clogging without water are preceded and no filter cake is formed at large pore size of soils. However, lowly permeable slurry candidates can achieve a thin filter cake formation owing to its clogging potential and low permeability.

Referred a guideline for drilling fluids, a minimum filtrate volume of 12.5 mL is recommended for bentonite slurries (American Petroleum Institute 2020). The test result of this study indicates B+XG and K+XG slurries to be feasible in terms of k, where the k of B+XG and K+XG slurries are similar or even lower than B7.5 (k = 1.92 × 10^{-6} m/s).

4.4 Suspended viscosity (η_{sus})

Suspended viscosity (η_{sus}) was measured to assess the transportation efficiency of slurry + excavated spoil (CS for coarse soil spoil, FS for fine soil spoil) mixtures. As pure K slurries (K2.5, K5.0, K7.5, and K10.0) are evaluated to be inappropriate in terms of η, τ_o, η_p, p_s, and k, pure bentonite (B-), B+XG, and K+XG slurries were considered for η_{sus} assessment.

The η_{sus} of the B10.0 slurry was unstable at lower shear rates regardless of the spoil configuration (20% CS and 10% FS) (Fig. 9(a)), while B7.5 slurry with spoil showed clear shear thinning behavior. Meanwhile, the value of η_{sus} with coarse soil spoil (20% CS — 20% spoil in a mass ratio to slurry blend) and that with fine soil spoil (10% FS) shows little difference. With the presence of XG, both B+XG (Fig. 9(b)) and K+XG (Fig. 9(c) — 10% spoil in a mass ratio to slurry blend) slurries show amended η_{sus} and shear thinning behavior, regardless of clay and spoil type and amount. Considering that velocity gradient perpendicularly to the flow attributes shear stress of supporting medium (Dias and Bezuijen 2015), the amended suspended viscosity may ensure stable applicability on lower shear rate than 0.1 s^{-1}.

4.5 Stickiness (λ)

As the objective of this study was to recommend the most effective slurry type while prioritizing the tunneling properties, competitive cases (B7.5, B10.0, B2.5-XG0.5,

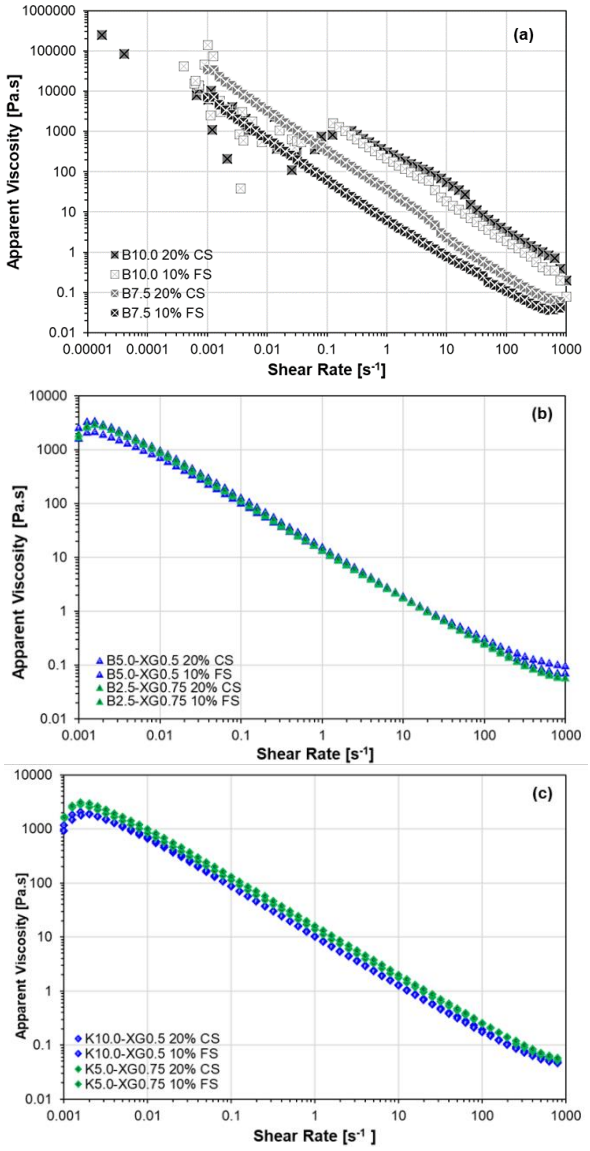

Fig. 9 Assessment of suspended viscosity (η_{sus}) using coarse soil and fine soil

B5.0-XG0.5, K5.0-XG0.75, and K10.0-XG0.5) were selected for stickiness (λ) assessment (Table 4). The λ values of B+XG and K+XG slurries were higher than the λ of B7.5 (λ = 0.15%) but considerably lower than that of B10.0 (λ = 1.47%). Experimental result implies λ of B+XG and K+XG slurries to be acceptable in practice when compared to the λ of B7.5.

Although the λ values of B+XG slurries and K+XG slurries are within acceptable ranges, the B+XG slurries were less effective, in terms of λ, than the K+XG slurries. This is because the higher λ is, the greater the adhesion or clogging of transportation system occurs. In fact, the B+XG slurries had a higher λ for the same XG content and a lower clay content than K+XG slurries. For instance, the λ value of K10.0-XG0.5 was 0.33%. This result indicates that even at a same XG content, the higher λ of B5.0-XG0.5 attributes to the surface characteristic of bentonite which has higher specific surface area and cation exchange capacity than

Table 4 Stickiness ratio (λ) assessment results obtained using empirical equation

Slurry type	Stickiness ratio, [%]
B10.0	1.47
B7.5	0.15
B5.0-XG0.5	0.55
B2.5-XG0.75	0.42
K10.0-XG0.5	0.33
K5.0-XG0.75	0.36

kaolinite clay. Thus, it is expected that reduction of bentonite amount leads to enhanced transportation performance and K+XG slurries also have greater potential in terms of λ.

5. Competitiveness evaluation via statistical analysis

This study aims to assess the technical feasibility of B+XG and K+XG slurries to substitute or reduce the use of common bentonite slurries in TBM excavation practices.

The competitiveness evaluation was performed for the B+XG and K+XG slurries considered in this study through statistical analysis using the data obtained via laboratory assessments. Inferential statistical methodology was used to improve reliability in practice. Inferential statistical methodology allows to make prediction from experimental assessment result (specimen data) to practical performance efficiency (population) (Guerrero 2019, Kalter *et al.* 1983). Fig. 10 describes the overall procedure of statistical analysis performed in this study. The experimental findings (i.e., η_p, τ_o, p_s, and k) were standardized using the matching property values of the B7.5 slurry (common slurry type) and set to be the input values (Table 5) for statistical analysis.

The inferential statistics were started using input data. x_i is a normalized property (input data) including the η_p, τ_o, p_s, and k, and the cost efficiency was optionally analyzed (①).

Each component of input data (x_i) was multiplied to random integer weight factor (w_i) between 1 to 10 (②) referring the orthogonal experimental design to apply multi-attribute (Pang *et al.* 2023). Since weight factor is a randomly selected integer between 1 to 10, 10^4 (considering 4 inputs) or 10^5 (considering 5 inputs) integer combinations of weight factors created the same number of y values. In detail, 105 weight factor combinations are generated when five input data (i.e., η_p, τ_o, p_s, k and cost efficiency) are considered, while 10^4 weight factor combinations analysis excludes the cost efficiency.

Intrinsic value (y_i) of each slurry candidate was derived from summation of weight factor-applied input data as follows (for Step (3) in Fig. 10):

$$y_i = w_1x_1 + w_2x_2 + w_3x_3 + w_4x_4 + (w_5x_5)$$

*Note: w_5 and x_5 are optional

The competitive value (z_i) was evaluated by comparison of intrinsic values (y_i) and that of B7.5, where B7.5

Table 5 Overall comparison chart

Slurry type	B10.0	B7.5	K10.0	K7.5	K10.0XG0.5	K5.0XG0.75	B5.0XG0.5	B2.5XG0.75
Plastic viscosity (η_p)	1.004	1.0	-	-	1.543	2.585	0.974	0.694
Yield point (τ_o)	11.429	1.0	-	-	0.571	0.571	0.214	2.800
Swelling (p_s)	1.3	1.0	-	-	0.07	0.11	0.667	0.667
Permeability (k)	1.580	1.0	0.0054	0.0037	0.001	0.001	0.001	0.001
Suspended viscosity (20% CS)	6.874	1.0	-	-	1.276	1.414	1.276	1.414
Suspended viscosity (10% FS)	5.597	1.0	-	-	3.573	8.784	2.979	1.849
Stickiness ratio	9.800	1.0	-	-	2.200	2.400	3.667	2.800
Price/ton [USD]	16.368	12.656	13.368	10.406	20.360	17.933	15.936	15.721
Cost efficiency	1.293	1.0	1.056	0.822	1.609	1.417	1.259	1.242

Table 6 Inferential statistical assessment

	Slurry type							
Tunneling properties	B7.5	B10.0	K10.0	K7.5	K10.0XG0.5	K5.0XG0.75	B5.0XG0.5	B2.5XG0.75
1st priority	-	0	0	0	710	4553	6	4731
2nd priority	-	0	0	0	1894	4952	573	2581
Tunneling properties with cost	B7.5	B10.0	K10.0	K7.5	K10.0XG0.5	K5.0XG0.75	B5.0XG0.5	B2.5XG0.75
1st priority	-	0	0	0	21612	41972	866	35550
2nd priority	-	0	0	1	34213	38947	5753	21086

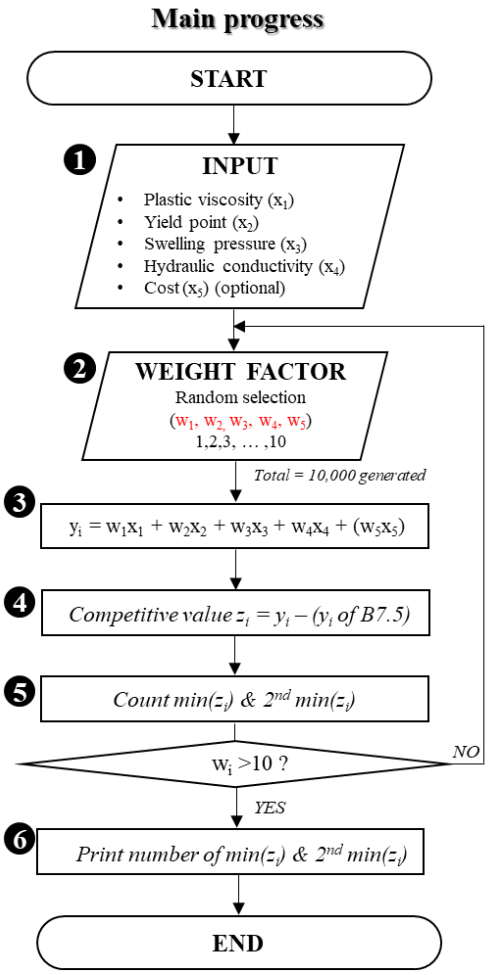

Fig. 10 Flow chart for inferential statistical analysis

represents the typical bentonite content (3% to 8%) of tunneling slurries used in practice (Swartz 2021).

Step 4: $z_i = y_i - y_i$ of B7.5

Under the assumption that smaller z value renders better performance which has similar properties to B7.5 slurry, the smallest and most next (i.e., second) smallest y values were respectively assigned to 1st-priority and 2nd-priority cases, respectively (⑤). The counts of 1st-priority and 2nd-priorty are listed in Table 6 (⑥).

For example, a random case having weight factor combinations as, $w_1 = 3$, $w_2 = 5$, $w_3 = 2$, $w_4 = 1$, and $w_5 = 1$ (for stage ② in Fig. 11) applied to input data is described in Fig. 11. For the input matrix (①in Fig. 10), each column represents the measured properties (η_p, τ_o, p_s, k, and the cost efficiency) while rows distinguish different slurry types. As a result, intrinsic values of each slurry candidate (③) are calculated with an allocated random weight factor combination. The competitive values (z_i) are calculated by comparison with that of B7.5 (④). K5.0-XG0.75 and K10.0-XG0.5 are computed to be the smallest (1st-priority) and next smallest (2nd-priority) cases, respectively (⑤). Both cases are counted in this weight factor combination. These overall progresses are repeated unless each weight factor exceeds 10.

Consequently, two slurries (B2.5-XG0.75 and K5.0-XG0.75) were evaluated as the most competitive slurry configurations (Table 6). When four tunneling properties (η_p, τ_o, p_s, and k) were considered, B2.5-XG0.75 and K5.0-XG0.75 cases were counted as the 1st-priority for 4731

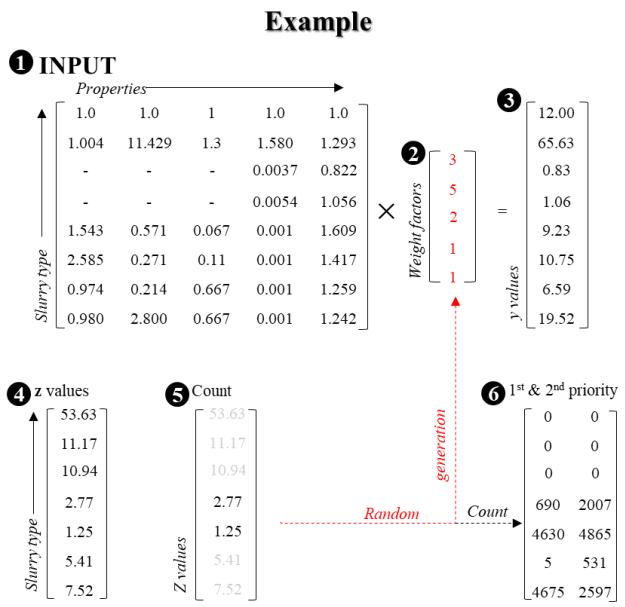

Fig. 11 Example of the inferential statistical analysis

times and 4553 times, respectively. Both cases composed 93% of total 1st-priority cases. Moreover, K5.0-XG0.75 became the predominant (49.52%) case for the 2nd-priority counts. When the cost (price/ton in USD) was additionally considered to statistical analysis, the K5.0-XG0.75 slurry showed the highest competitiveness by counting 41972 and 38947 for the 1st-priority and 2nd-priority cases of subsidiary cases.

Even though statistical analysis was performed by inferential statistical analysis, which speculates numbers of cases from population, random weight factor application redeemed limitation of inferential statistics. In conclusion, B2.5-XG0.75 and K5.0-XG0.75 are expected to enhance environmental sustainability by reduction of bentonite clay content. The possibility of K+XG slurries was also confirmed from this statistical approach.

6. Conclusions

This research aims to investigate the viability of utilizing sustainable slurry alternatives, specifically kaolinite clay and XG (xanthan gum), in lieu of polymer additives to diminish the reliance on bentonite in tunnel excavation using the Slurry Shield Tunnel Boring Machine (SS TBM). The extensive use of bentonite as a slurry poses environmental concerns due to its high adsorption capacity, leading to potential hazards upon disposal. The evaluation focused on the permeability, rheological properties, and swelling characteristics of the slurries concerning tunneling performance, as well as suspended viscosity and stickiness in terms of muck transport efficiency. Experimental assessments revealed that kaolinite clay alone exhibited unstable rheological behavior, posing potential safety risks and higher construction costs. However, combinations of bentonite with XG (B+XG) and kaolinite clay with XG (K+XG) displayed promising results in laboratory testing. Given that these properties collectively influence TBM excavation efficiency, a probabilistic approach employing random weight factors was applied in this study. Inferential statistical analysis with tunneling properties indicated both B2.5-XG0.75 (with 47.31% priority) and K5.0-XG0.75 (with 45.53% priority) as competitive and feasible alternatives compared to conventional B7.5 slurry. Furthermore, considering economic feasibility, K5.0-XG0.75 was identified as the most practical slurry condition for implementation. Consequently, this study underscores the effectiveness of using xanthan gum biopolymer as an additive in bentonite-based TBM slurries and suggests the potential adoption of kaolinite clay-xanthan gum mixtures as alternative slurry materials for TBM excavation in the future. Given the potential of xanthan gum biopolymer, a practical assessment should be conducted as a subsequent study before proceeding with implementation.

Acknowledgments

This work was supported by the National Research Foundation of Korea (NRF) grant funded by the Korea government (MSIT) (No. 2022R1A2C2091517), and the Korea Agency for Infrastructure Technology Advancement (KAIA) grant funded by the Ministry of Land, Infrastructure and Transport (Grant RS-2021-KA163162) and Korea Electric Power Corporation (Grant R23SG01).

References

Alther, G.R. (1987), "The qualifications of bentonite as a soil sealant", *Eng. Geol.*, **23**(3-4), 177-191. https://doi.org/10.1016/0013-7952(87)90089-5.

American Petroleum Institute (2020), "API Specification 13A", *Drilling Fluids Materials*, Washington, DC, USA.

ASTM (2015), *D7175-15: Determining the Rheological Properties of Asphalt Binder Using a Dynamic Shear Rheometer*, ASTM International, West Conshohoken, PA. https://doi.org/10.1520/d7175-15.

ASTM (2021), *D4546-21: Standard test methods for one-dimensional swell or collapse of soils*, ASTM International, West Conshohocken, PA. https://doi.org/10.1520/d4546-21.

Bernard, H., Lau, M., Senthilkumar, M., Sze, Y., Marotta, M., Ow, C. and Senthilnath, G. (2019), "High density slurry for shallow bored tunneling in Singapore", *Tunnels and Underground Cities: Engineering and Innovation Meet Archaeology, Architecture and Art.* CRC Press, 5350-5359. https://doi.org/10.1201/9780429424441-566.

Blkoor, S.O. and Fattah, K.A. (2013), "The influence of XC-polymer on drilling fluid filter cake properties and formation damage", *J. Pet. Environ. Biotechnol.*, **4**(5). https://doi.org/10.4172/2157-7463.1000157.

Broni-Bediako, E. and Amorin, R. (2010), "Effects of drilling fluid exposure to oil and gas workers presented with major areas of exposure and exposure indicators", *Res. J. Appl. Sci. Eng. Technol.*, **2**(8), 710-719.

Cabalar, A.F., Wiszniewski, M. and Skutnik, Z. (2017), "Effects of xanthan gum biopolymer on the permeability, odometer, unconfined compressive and triaxial shear behavior of a sand", *Soil Mech. Found. Eng.*, **54**(5), 356-361. https://doi.org/10.1007/s11204-017-9481-1.

Chang, I. and Cho, G.C. (2019), "Shear strength behavior and parameters of microbial gellan gum-treated soils: from sand to clay", *Acta Geotechnica*, **14**(2), 361-375. https://doi.org/10.1007/s11440-018-0641-x.

Chang, I., Im, J. and Cho, G.C. (2016), "Introduction of microbial biopolymers in soil treatment for future environmentally-friendly and sustainable geotechnical engineering", *Sustainability*, **8**(3), 251. https://doi.org/10.3390/su8030251.

Chang, I., Im, J., Prasidhi, A K. and Cho, G.C. (2015), "Effects of xanthan gum biopolymer on soil strengthening", *Constr. Build. Mater.*, **74**, 65-72. https://doi.org/10.1016/j.conbuildmat.2014.10.026.

Chang, I., Kwon, Y.M. and Cho, G.C. (2021), "Effect of pore-fluid chemistry on the undrained shear strength of xanthan gum biopolymer-treated clays", *J. Geotech. Geoenviron. Eng.*, **147**(11), 06021013. https://doi.org/10.1061/(ASCE)GT.1943-5606.0002652.

Chang, I., Kwon, Y.M., Im, J. and Cho, G.C. (2019), "Soil consistency and interparticle characteristics of xanthan gum biopolymer–containing soils with pore-fluid variation", *Can. Geotech. J.*, **56**(8), 1206-1213. https://doi.org/10.1139/cgj-2018-0254.

Chang, I., Lee, M., Tran, A. T.P., Lee, S., Kwon, Y.M., Im, J. and Cho, G.C. (2020), "Review on biopolymer-based soil treatment (BPST) technology in geotechnical engineering practices", *Transport. Geotech.*, **24**, 100385. http://doi.org/10.1016/j.trgeo.2020.100385.

Cui, J., Xu, W.H., Fang, Y., Tao, L.M. and He, C. (2020a), "Performance of slurry shield tunnelling in mixed strata based on field measurement and numerical simulation", *Adv. Mater. Sci. Eng.*, 2020. https://doi.org/10.1155/2020/6785260.

Cui, W., Liu, D., Song, H.F., Zhang, S.R. and He, S.W. (2020b), "Experimental study of salt-resisting slurry for undersea shield tunnelling", *Tunn. Undergr. Sp. Tech.*, **98**, 103322. https://doi.org/10.1016/j.tust/2020.103322.

Dias, T.G.S. and Bezuijen, A. (2015), "TBM pressure models–observations, theory and practice", *Proceedings of the 15th Pan-American Conference on Soil Mechanics and Geotechnical Engineering-Geotechnical Synergy in Buenos Aires*, Buenos Aires, November.

Dorman, D.C., Foster, M.L., Olesnevich, B., Bolon, B., Castel, A., Sokolsky-Papkov, M. and Mariani, C.L. (2018), "Toxicity associated with ingestion of a polyacrylic acid hydrogel dog pad", *J. Veterinary Diagnostic Investigation*, **30**(5), 708-714. https://doi.org/10.1177/1040638718782583.

Feinendegen, M., Ziegler, M., Spagnoli, G., Fernández-Steeger, T., and Stanjek, H. (2010), "A new laboratory test to evaluate the problem of clogging in mechanical tunnel driving with EPB-shields", *Rock Mech. Civil Environ. Eng.*, 429-432. https://doi.org/10.1201/b10550-101.

Fritz, P. (2007), "Additives for slurry shields in highly permeable ground", *Rock Mech. Rock Eng.*, **40**(1), 81-95. https://doi.org/10.1007/s00603-006-0090-y.

Fu, W., Chen, B., Zhang, K., Liu, J., Sun, X., Huang, B. and Sun, B. (2022), "Rheological Behavior of Hydrate Slurry with Xanthan Gum and Carboxmethylcellulose under High Shear Rate Conditions", *Energ. Fuel.*, **36**(6), 3169-3183. https://doi.org/10.1021/acs.energyfuels.1c04359.

García-Ochoa, F., Santos, V., Casas, J., and Gomez, E. (2000), "Xanthan gum: production, recovery, and properties", *Biotechnology advances*, **18**(7), 549-579. https://doi.org/10.1016/s0734-9750(00)00050-1.

Gardner, R.O.N. (2003), "Overview and characteristics of some occupational exposures and health risks on offshore oil and gas installations", *Annal. Occupational Hygiene*, **47**(3), 201-210. https://doi.org/10.1093/annhyg/meg028.

Guerrero, H. (2019), "Inferential statistical analysis of data", *Excel Data Analysis: Modeling and Simulation*, 179-224. https://doi.org/10.1007/978-3-642-10835-8_6.

Holtz, R.D., Kovacs, W.D. and Sheahan, T.C. (2011), *An introduction to geotechnical engineering*, Pearson, Upper Saddle River, NJ.

Jain, A.K. (2024), "Exploring the viability of Bentonite-amended blends incorporating marble dust, sand and fly ash for the creation of an environmentally sustainable landfill liner system", *Int. J. Geo-Eng.*, **15**(1), 16.

Kalter, N., Feinberg, M. and Carroll, B.J. (1983), "Inferential statistical methods for strengthening the interpretation of laboratory test results", *Psychiatry Res.*, **10**(3), 207-216. https://doi.org/10.1016/0165-1781(83)90057-4.

Katzbauer, B. (1998), "Properties and applications of xanthan gum", *Polymer Degradation and Stability*, **59**(1), 81-84. http://doi.org/10.1016/s0141-3910(97)00180-8.

Kelessidis, V.C., Tsamantaki, C., Pasadakis, N., Repouskou, E. and Hamilaki, E. (2007), "Permeability, porosity and surface characteristics of filter cakes from water–bentonite suspensions", *WIT T. Eng. Sci.*, **56**, 173-182. https://doi.org/10.2495/MPF070171.

Krause, T. (1987), "Schildvortrieb mit fl€ uussigkeitsund erdgest€ uutzter Ortsbrust", Ph.D. Dissetation, Technical University of Braunschsweig, Braunschsweig, Germany.

Kubilay, Ş., Gürkan, R., Savran, A. and Şahan, T. (2007), "Removal of Cu (II), Zn (II) and Co (II) ions from aqueous solutions by adsorption onto natural bentonite", *Adsorption*, **13**(1), 41-51. https://doi.org/10.1007/s10450-007-9003-y.

Kwon, Y.M., Cho, G.C., Chung, M. and Chang, I. (2021), "Surface erosion behavior of biopolymer-treated river sand", *Geomech. Eng.*, **25**(1), 49-58. https://doi.org/10.12989/gae.2021.25.1.049.

Latifi, N., Horpibulsuk, S., Meehan, C.L., Majid, M.Z.A. and Rashid, A.S.A. (2016), "Xanthan gum biopolymer: an eco-friendly additive for stabilization of tropical organic peat", *Environ. Earth Sci.*, **75**(9), 825. https://doi.org/10.1007/s12665-016-5643-0.

Lee, M., Im, J., Cho, G.C., Ryu, H.H. and Chang, I. (2021), "Interfacial shearing behavior along Xanthan gum biopolymer-treated sand and solid interfaces and its meaning in geotechnical Engineering aspects", *Appl. Sci.*, **11**(1), 139. http://doi.org/10.3390/app11010139.

Lee, S., Chang, I., Chung, M.K., Kim, Y. and Kee, J. (2017), "Geotechnical shear behavior of xanthan gum biopolymer treated sand from direct shear testing", *Geomech. Eng.*, **12**(5), 831-847. https://doi.org/10.12989/gae.2017.12.5.831.

Lee, S., Chung, M., Park, H.M., Song, K.I. and Chang, I. (2019), "Xanthan gum biopolymer as soil-Stabilization binder for road construction using local soil in Sri Lanka", *J. Mater. Civil Eng.*, **31**(11), 06019012. https://doi.org/10.1061/(ASCE)MT.1943-5533.0002909.

Lee, S., Im, J., Cho, G.C. and Chang, I. (2019), "Laboratory triaxial test behavior of xanthan gum biopolymer-treated sands", *Geomech. Eng.*, **17**(5), 445-452. https://doi.org/10.12989/gae.2019.17.5.445.

Liu, M., Liao, S., Shi, Z., Liu, H. and Chen, L. (2023), "Analytical study and field investigation on the effects of clogging in slurry shield tunneling", *Tunn. Undergr. Sp. Tech.*, **133**, 104957.

Malusis, M.A. and McKeehan, M.D. (2013), "Chemical compatibility of model soil-bentonite backfill containing multiswellable bentonite", *J. Geotech. Geoenviron. Eng.*, **139**(2), 189-198. https://doi.org/10.1061/(ASCE)GT.1943-5606.0000729.

Min, F., Zhu, W. and Han, X. (2013), "Filter cake formation for slurry shield tunneling in highly permeable sand", *Tunn.*

Undergr. Sp. Tech., **38**, 423-430. https://doi.org/10.1016/j.tust.2013.07.024.

Mooney, M. (1951), "The viscosity of a concentrated suspension of spherical particles", *J. Colloid Sci.*, **6**(2), 162-170. http://doi.org/10.1016/0095-8522(51)90036-0.

N'gouamba, E., Essadik, M., Goyon, J., Oerther, T. and Coussot, P. (2021), "Yielding and rheopexy of aqueous xanthan gum solutions", *Rheologica Acta*, **60**(11), 653-660. https://doi.org/10.1007/s00397-021-01293-1.

New Jersey Department of Health (2016), "Hazardous substance face sheet - sulfuric acid", New Jersey Department of Health.

Ong, E.E., O'Byrne, S. and Liow, J.L. (2019), "Yield stress measurement of a thixotropic colloid", *Rheologica Acta*, **58**, 383-401. https://doi.org/10.1007/s00397-019-01154-y.

Ouhadi, V.R., Yong, R.N. and Sedighi, M. (2006), "Influence of heavy metal contaminants at variable pH regimes on rheological behaviour of bentonite", *Appl. Clay Sci.*, **32**(3-4), 217-231. https://doi.org/10.1016/j.clay.2006.02.003.

Pang, J., Zhang, X. and Zhang, B. (2023), "Orthogonal experimental study on the construction of a similar material proportional model for simulated coal seam sampling", *Processes*, **11**, 2125.

Park, B., Chang, S.H., Choi, S.W. and Lee, C. (2020), "A study for the estimation of TBM design parameters by statistical analysis", *Geotechnics for Sustainable Infrastructure Development*, 355-360. https://doi.org/10.1007/978-981-15-2184-3_45.

Park, H., Oh, J.Y., Kim, D. and Chang, S. (2018), "Monitoring and analysis of ground settlement induced by tunnelling with slurry pressure-balanced tunnel boring machine", *Adv. Civil Eng.*, **2018**, 5879402. https://doi.org/10.1155/2018/5879402.

Peila, D., Picchio, A., Martinelli, D. and Dal Negro, E. (2016), "Laboratory tests on soil conditioning of clayey soil", *Acta Geotechnica*, **11**(5), 1061-1074. http://doi.org/10.1007/s11440-015-0406-8.

Phillips, G.O. and Williams, P.A. (2000), Handbook of hydrocolloids, CRC Press.

Rankine, B.R. (2007), "Assessment and analysis of Queensland clay behavior", Ph.D. Dissertation, James Cook University, Douglas QLD, Australia.

Rostami, J., Hassanpour, J. and Samadi, H. (2023), "Prediction of earth pressure balance for EPB-TBM using machine learning algorithms", *Int. J. Geo-Eng.*, **14**(1), 21.

Shirlaw, J.N., Yan, Z. and Xiao, X.C. (2009), "Assessing face pressures for slurry shield tunneling through partially dewatered weathered gneiss", *Underground Singapore*.

Simha, R. (1952), "A treatment of the viscosity of concentrated suspensions", *J. Appl. Phys.*, **23**(9), 1020-1024. https://doi.org/10.1063/1.1702338.

Sun, B.P., Zhao, B., Cao, H., Wang, J., Mo, D. and Zhang, S. (2018), "Lab study on the effect of cation exchange capacity on slurry performance in slurry shields", *Adv. Civil Eng.*, 2018. https://doi.org/10.1155/2018/2942576.

Swartz, S. (2021), "MDOT Question on slurry containment : slurry systems with excavation by TBM", Michigan Department of Transportation.

The French Association of Tunnels and Underground Space, A. (2005), "AFTES Recommendation - Slurry for use in Slurry Shield TBM".

Thomas, D.G. (1965), "Transport characteristics of suspension: VIII. A note on the viscosity of Newtonian suspensions of uniform spherical particles", *J. Colloid Sci.*, **20**(3), 267-277. https://doi.org/10.1016/0095-8522(65)90016-4.

Yoon, S., Jeon, J.S., Chang, S., Lee, D.H., Lee, S.R. and Kim, G.Y. (2020), "Characteristics of water suction for a Korean compacted bentonite", *Nuclear Technol.*, **206**(3), 514-525. https://doi.org/10.1080/00295450.2019.1632093.

Yoshida, Y., Katsumoto, T., Taniguchi, S., Shimosaka, A., Shirakawa, Y. and Hidaka, J. (2013), "Prediction of viscosity of slurry suspended fine particles using coupled DEM-DNS simulation", *Chem. Eng. Transact.*, **32**, 2089-2094. https://doi.org/10.3033/CET1332349.

Zhao, S., Li, S., Wan, Z. and Wang, M. (2021), "Dispersant for reducing mud cakes of slurry shield tunnel boring machine in sticky ground", *Adv. Mater. Sci. Eng.*, 2021, 1-10. https://doi.org/10.1155/2021/5524489.

Zumsteg, R., Puzrin, A.M. and Anagnostou, G. (2016), "Effects of slurry on stickiness of excavated clays and clogging of equipment in fluid supported excavations", *Tunn. Undergr. Sp. Tech.*, **58**, 197-208. https://doi.org/10.1016/j.tust.2016.05.006.

IC